Supporting Information

Molecular Dynamics Insights into Orientation and Hexagonal Ordering of Tripodal Triptycenes on Solid Surfaces

Kaito Nitta,[a] *Yoshiaki Shoji,*[b,c] *Takanori Fukushima*[b,c] *and Go Watanabe*[a,d]*

a. Department of Physics, School of Science, Kitasato University, 1-15-1 Kitazato, Minami-ku, Sagamihara, Kanagawa 252-0373, Japan

b. Laboratory for Chemistry and Life Science, Institute of Integrated Research, Institute of Science Tokyo, 4259 Nagatsuta, Midori-ku, Yokohama 226-8501, Japan

c. Research Center for Autonomous Systems Materialogy (ASMat), Institute of Integrated Research, Institute of Science Tokyo, 4259 Nagatsuta, Midori-ku, Yokohama 226-8501, Japan

d. Department of Data Science, School of Frontier Engineering, Kitasato University, 1-15-1 Kitazato, Minami-ku, Sagamihara, Kanagawa 252-0373, Japan

Corresponding Author

Go Watanabe: go0325@kitasato-u.ac.jp

Simulation details

The initial bulk structure of Trip1 was created by stacking 8, 9, and 4 unit cells of the crystal structure in the *x*, *y*, and *z* directions, respectively, including a total of 576 molecules (Figure S1). To construct the bulk structure with neighboring molecules in an antiparallel alignment, one molecule in the unit cell was inverted, and the same procedure was applied. The initial structures of Trip2 and Trip3 were constructed by replacing the corresponding molecules in the initial structure of Trip1 with those of Trip2 and Trip3, respectively. For the initial thin film structures, monolayers were constructed by placing 8 and 9 unit cells in the *x* and *y* directions, respectively, yielding 144 triptycene derivatives per monolayer. Thin films of 2, 3, and 4 layers were created by stacking these monolayers in the *z* direction, with 5 nm thick blank cells placed above and below these layers. Tables S1 and S2 summarize the parameters specifying the dimensions and shape of the initial MD simulation cell for the bulk system and thin films with 1–4 layers, respectively.

The initial structures of the monolayers of Trip1, Trip2, and Trip3 aligned in parallel and antiparallel arrangements placed at the interface of an SiO_2 layer were prepared according to the procedure described above, and the SiO_2 substrate was generated based on previous reports[S1,S2,S3]. The substrate contained 2530, 506, and 506 units of SiO_2, SiO_2(OH), and SiO(OH), respectively, with a thickness of 1.9912 nm. In the substrate-based systems, the monolayers were also sandwiched between two 5 nm thick blank cells, and the dimensions and shape parameters of the initial MD simulation cell are listed in Tables S3 and S4.

All-atom molecular dynamics (MD) simulations were performed using GROMACS 2020.5, which is a free program for fast and large-scale simulations. For the force field parameters used to calculate the intra- and intermolecular interactions of Trip1, Trip2, and Trip3, the generalized Amber force field[S4] parameters, which are widely used for accurate MD simulations of diverse systems, were applied. The Clay force field parameters[S5] were used for the Si and O atoms in the solid substrate. The partial atomic charges of the simulated triptycene derivatives were obtained using the restrained electrostatic potential (RESP) method,[S6] based on single point density functional theory (DFT) calculations performed with the Gaussian 16 revision C01 package[S7] at the B3LYP/6-31G(d,p) level of theory.

MD simulations for the molecular assemblies on the SiO_2 substrate were conducted under NVT ensemble. For both the bulk and thin-film systems, except for the stair-stepping trilayers on the SiO_2 substrate, pre-equilibration runs consisted of 5 ns NVT ensemble simulations at 250 K and 300 K, conducted sequentially. The temperature was kept using the Berendsen thermostat[S8], respectively, with relaxation times of 0.2 ps. Following pre-equilibration, 100 ns equilibration runs at 300 K were carried out using the Nosé-Hoover thermostat,[S9,S10] with relaxation times of 1.0 ps. The volume of the MD cell was fixed during both pre-equilibration and equilibration simulations. For the stair-stepping trilayers on the SiO_2 substrate, pre-equilibration runs were successively performed for 5 ns at 300 K and 400 K, followed by an equilibration run for 1,000 ns at 400 K. For all simulations, the time step was set to 2 fs and all covalent bonds connected to hydrogen atoms were constrained using the LINCS algorithm[S11]. Long-range electrostatic interactions were treated using the smooth particle mesh Ewald

method with a real-space cutoff of 1.2 nm and a Fourier spacing of 0.30 nm. The cutoff for the van der Waals interactions was set to 1.2 nm.

To compare the temperature dependence of thermal stability, we calculated *B*-factors[S12], which represent thermal atomic fluctuations, as expressed below:

$$B = \frac{8}{3}\pi^2\Delta_i^2 \quad (1)$$

where Δ_i is the root-mean-square fluctuations (RMSF) of atom i. The RMSF values are estimated using the following equation:

$$\Delta_i = \sqrt{\frac{1}{T}\sum_{j=1}^{T}\left|r_i(t_j) - \overline{r_i}\right|^2} \quad (2)$$

where T is the number of steps, $r_i(t_j)$ is the position coordinate of atom i at time t_j, and $\overline{r_i}$ is the average position atom i during T. The RMSF values were analyzed from MD simulation trajectories during the last 5 ns of the 100 ns equilibration.

Initial structures for the simulated systems

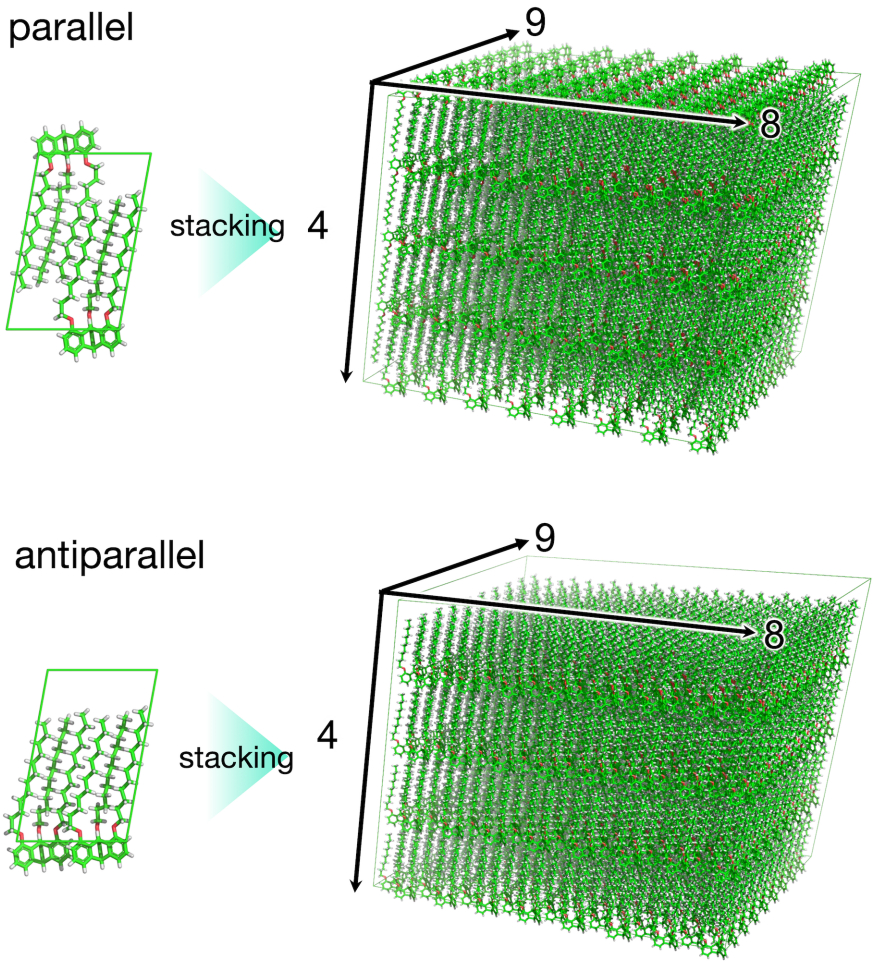

Figure S1. Initial structures of the bulk structure created by stacking 8, 9, and 4 unit cells of the crystal structure with respect to the *x*, *y*, and *z* directions, respectively. While the molecules in the bulk structure shown in the top are aligned in parallel, those shown in the bottom are aligned in antiparallel.

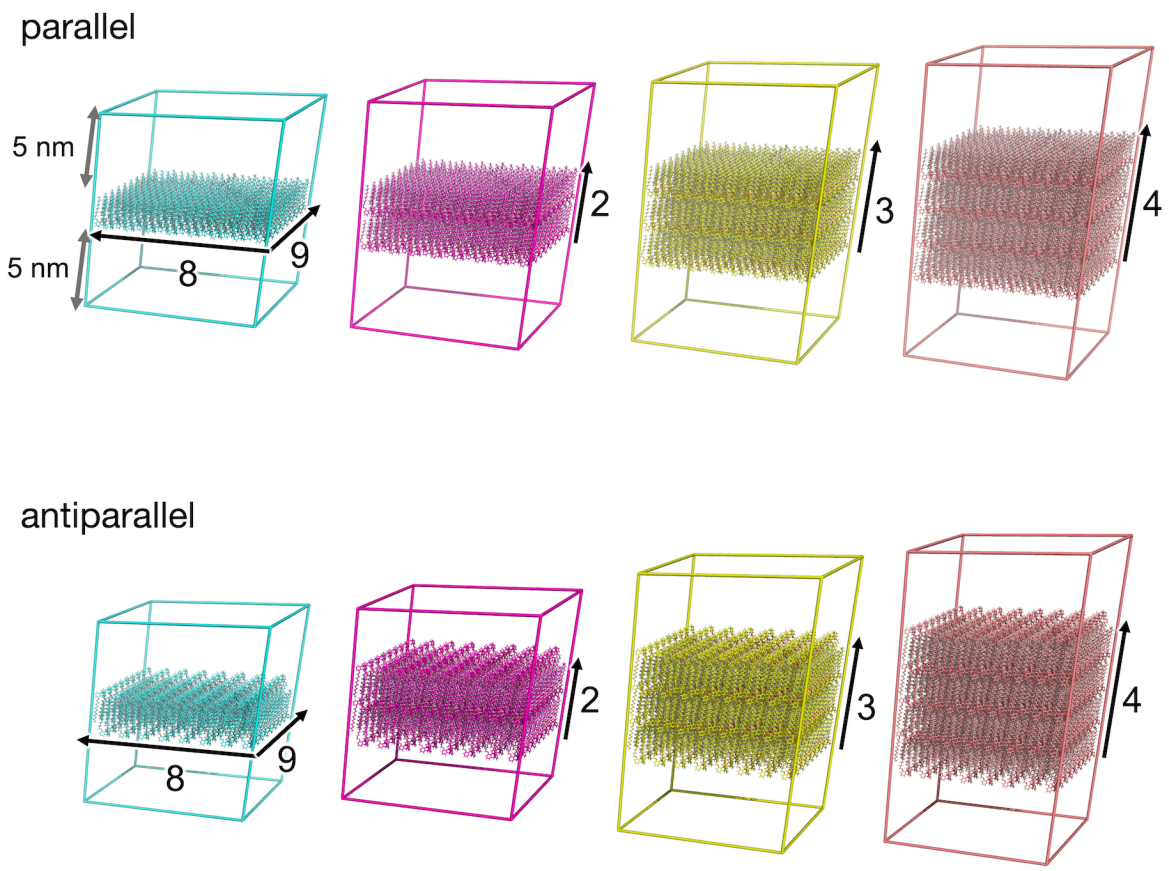

Figure S2. Initial structures of monolayer, 2 layers, 3 layers, and 4 layers colored by cyan, magenta, yellow, and pink. Monolayer was constructed by placing 8 and 9 unit cells in the same plane with respect to the *x* and *y* directions, respectively, and 2, 3, and 4 layers films were created by stacking monolayers in the *z* direction. 5 nm thick blank cells were placed above and below films.

Parameters specifying the initial MD simulation cells

Table S1. Parameters specifying the dimensions and shape of the initial MD simulation cell for the bulk system.

a (nm)	b (nm)	c (nm)	α (deg.)	β (deg.)	γ (deg.)
11.1443	7.2184	8.8684	90.00	100.28	90.00

Table S2. Parameters specifying the dimensions and shape of the initial MD simulation cell for thin films with 1–4 layers.

Number of layers	a (nm)	b (nm)	c (nm)	α (deg.)	β (deg.)	γ (deg.)
1	11.1443	7.2184	12.2171	90.00	100.28	90.00
2	11.1443	7.2184	14.4342	90.00	100.28	90.00
3	11.1443	7.2184	16.6513	90.00	100.28	90.00
4	11.1443	7.2184	18.8684	90.00	100.28	90.00

Table S3. Parameters specifying the dimensions and shape of the initial MD simulation cell for a monolayer on an SiO_2 substrate.

a (nm)	b (nm)	c (nm)	α (deg.)	β (deg.)	γ (deg.)
11.4494	7.6428	14.0000	90.000	90.000	90.00

Table S4. Parameters specifying the dimensions and shape of the initial MD simulation cell for a stair-stepping trilayer on an SiO_2 substrate.

a (nm)	b (nm)	c (nm)	α (deg.)	β (deg.)	γ (deg.)
11.4494	7.6428	19.0000	90.000	90.000	90.00

MD simulation snapshots for the simulated systems

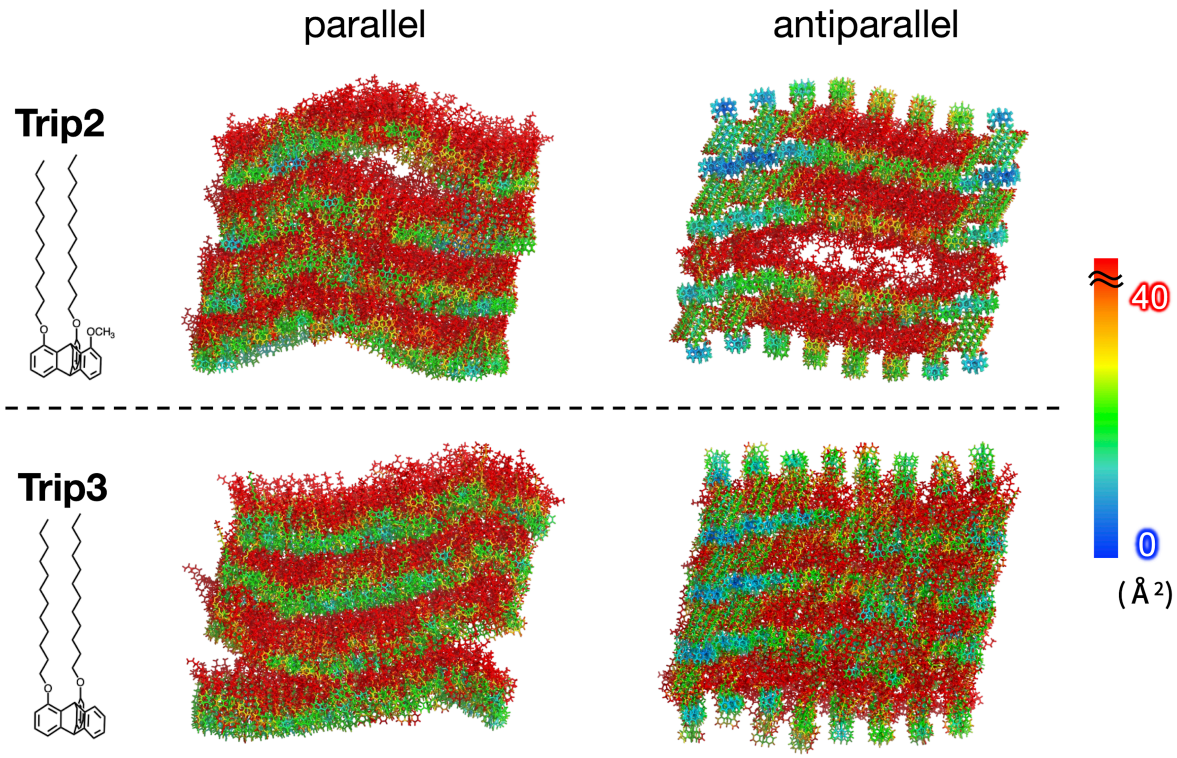

Figure S3. MD simulation snapshots with color-coded *B*-factor distributions for parallel (left) and antiparallel (right) molecular alignment systems of Trip2 and Trip3 after the 100 ns equilibration run at 300 K. Atoms are color-coded using a rainbow scale for values of *B*-factor ranging from 0 to 40 Å^2, while all values exceeding 40 are represented in red.

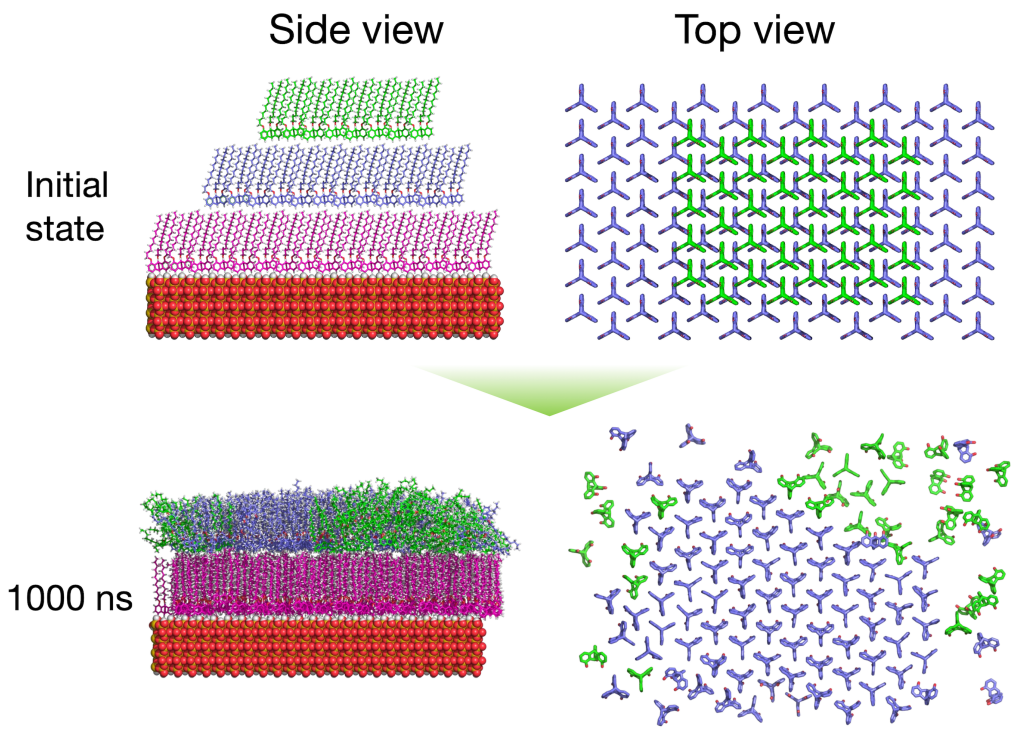

Figure S4. MD simulation snapshots of the stair-stepping trilayer of Trip1 on the SiO_2 substrate during the annealing process. (left) Side views of the entire trilayer and substrate, and (right) top views focusing on the triptycene moieties within the upper two layers.

Hexatic order parameter

The hexatic order parameter $\psi_6(\boldsymbol{r}_k)$ at a given time is defined as

$$\psi_6(\boldsymbol{r}_k) = \frac{1}{6}\sum_{j=1}^{6} \boldsymbol{e}^{i6\theta_{kj}(\boldsymbol{r}_k)}$$

where the triptycene molecule j is one of the six nearest neighbors of molecule k within 0.9 nm, and $\theta_{kj}(\boldsymbol{r_k})$ is the angle between a reference axis $\boldsymbol{e}$ and the vector connecting molecules k and j.

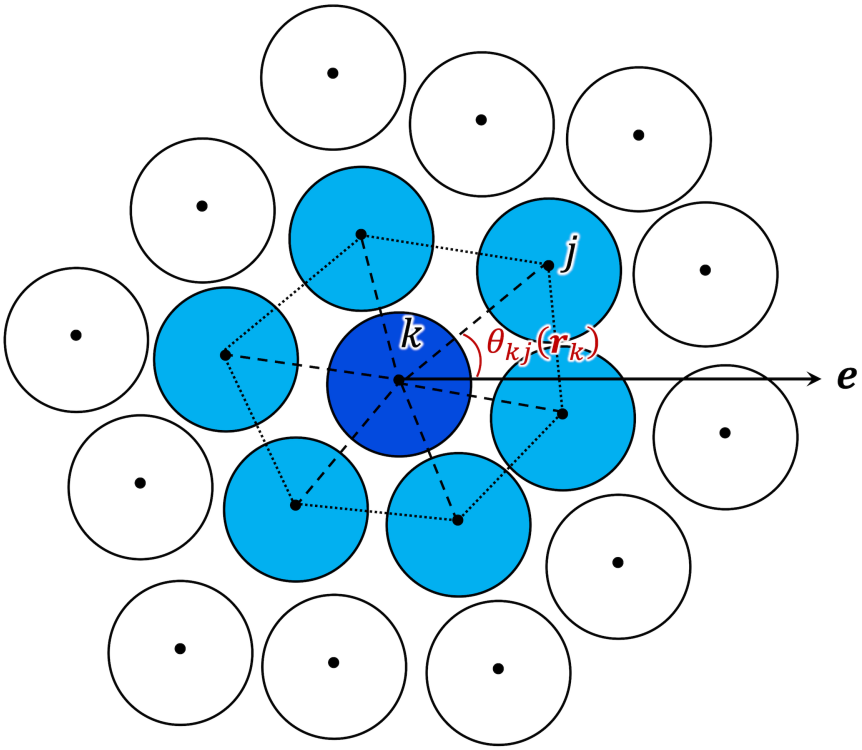

Figure S5. Schematic illustration showing molecule k, its six nearest neighbors, the reference axis $\boldsymbol{e}$, and the angle $\theta_{kj}(\boldsymbol{r_k})$ between $\boldsymbol{e}$ and the vector connecting molecules k and j.

References

[S1] T. Okamoto, M. Mitani, C. P. Yu, C. Mitsui, M. Yamagishi, H. Ishii, G. Watanabe, S. Kumagai, D. Hashizume, S. Tanaka, M. Yano, T. Kushida, H. Sato, K. Sugimoto, T. Kato and J. Takeya, *J. Am. Chem. Soc.*, 2020, **142**, 14974–14984.

[S2] O. Kroutil, Z. Chval, A. A. Skelton and M. Předota, *J. Phys. Chem. C*, 2015, **119**, 9274–9286.

[S3] T. Wei, M. S. J. Sajib, M. Samieegohar, H. Ma and K. Shing, *Langmuir*, 2015, **31**, 13543–13552.

[S4] J. Wang, R. M. Wolf, J. W. Caldwell, P. A. Kollman and D. A. Case, *J. Comput. Chem.*, 2004, **25**, 1157–1174.

[S5] R. T. Cygan, J. J. Liang and A. G. Kalinichev, *J. Phys. Chem. B*, 2004, **108**, 1255–1266.

[S6] C. I. Bayly, P. Cieplak, W. D. Cornell and P. A. Kollman, *J. Phys. Chem.*, 1993, **97**, 10269–10280.

[S7] M. J. Frisch, G. W. Trucks, H. B. Schlegel, G. E. Scuseria, M. A. Robb, J. R. Cheeseman, G. Scalmani, V. Barone, G. A. Petersson, H. Nakatsuji, X. Li, M. Caricato, A. V. Marenich, J. Bloino, B. G. Janesko, R. Gomperts, B. Mennucci, H. P. Hratchian, J. V. Ortiz, A. F. Izmaylov, J. L. Sonnenberg, D. Williams-Young, F. Ding, F. Lipparini, F. Egidi, J. Goings, B. Peng, A. Petrone, T. Henderson, D. Ranasinghe, V. G. Zakrzewski, J. Gao, N. Rega, G. Zheng, W. Liang, M. Hada, M. Ehara, K. Toyota, R. Fukuda, J. Hasegawa, M. Ishida, T. Nakajima, Y. Honda, O. Kitao, H. Nakai, T. Vreven, K. Throssell, J. A. Montgomery, Jr., J. E. Peralta, F. Ogliaro, M. J. Bearpark, J. J. Heyd, E. N. Brothers, K. N. Kudin, V. N. Staroverov, T. A. Keith, R. Kobayashi, J. Normand, K. Raghavachari, A. P. Rendell, J. C. Burant, S. S. Iyengar, J. Tomasi, M. Cossi, J. M. Millam, M. Klene, C. Adamo, R. Cammi, J. W. Ochterski, R. L. Martin, K. Morokuma, O. Farkas, J. B. Foresman and D. J. Fox, Gaussian 16, Revision A.03, Gaussian, Inc., Wallingford CT, 2016.

[S8] H. J. C. Berendsen, J. P. M. Postma, W. F. Van Gunsteren, A. Dinola and J. R. Haak, *J. Chem. Phys.*, 1984, **81**, 3684–3690.

[S9] S. Nosé, *Mol. Phys.*, 1984, **52**, 255–268.

[S10] W. G. Hoover, *Phys. Rev. A*, 1985, **31**, 1695–1697.

[S11] B. Hess, H. Bekker, H. J. C. Berendsen and J. G. E. M. Fraaije, *J. Comput. Chem.*, 1997, **18**, 1463–1472.

[S12] T. Okamoto, S. Kumagai, E. Fukuzaki, H. Ishii, G. Watanabe, N. Niitsu, T. Annaka, M. Yamagishi, Y. Tani, H. Sugiura, T. Watanabe, S. Watanabe and J. Takeya, *Sci. Adv.*, 2020, **6**, eaaz0632.